

IKZF1 gene deletions drive resistance to cytarabine in B-cell precursor acute lymphoblastic leukemia

Britt M. T. Vervoort,^{1*} Miriam Butler,^{1*} Kari J.T. Grünewald,¹ Dorette S. van Ingen Schenau,¹ Trisha M. Tee,¹ Luc Lucas,² Alwin D. R. Huitema,^{1,3} Judith M. Boer,¹ Beat C. Bornhauser,⁴ Jean-Pierre Bourquin,⁴ Peter M. Hoogerbrugge,¹ Vincent H.J. van der Velden,⁵ Roland P. Kuiper,^{1,6} Laurens T. van der Meer^{1#} and Frank N. van Leeuwen^{1#}

¹Princess Máxima Center for Pediatric Oncology, Utrecht, the Netherlands; ²Netherlands Cancer Institute, Amsterdam, the Netherlands; ³Department of Clinical Pharmacy, University Medical Center Utrecht, Utrecht University, Utrecht, the Netherlands; ⁴Department of Pediatric Oncology, Children's Research Center, University Children's Hospital Zürich, Zürich, Switzerland; ⁵Department of Immunology, Erasmus MC, University Medical Center Rotterdam, Rotterdam, the Netherlands and ⁶Department of Genetics, Utrecht University Medical Center, Utrecht University, Utrecht, the Netherlands

*BMTV and MB contributed equally as first authors.

#LTvdM and FNvL contributed equally as senior authors.

Correspondence: F.N. van Leeuwen
F.N.vanleeuwen@prinsesmaximacentrum.nl

Received: September 23, 2023.

Accepted: May 22, 2024.

Early view: June 6, 2024.

<https://doi.org/10.3324/haematol.2023.284357>

©2024 Ferrata Storti Foundation

Published under a CC BY-NC license



Abstract

IKZF1 deletions occur in 10-15% of patients with B-cell precursor acute lymphoblastic leukemia (BCP-ALL) and predict a poor outcome. However, the impact of *IKZF1* loss on sensitivity to drugs used in contemporary treatment protocols has remained underexplored. Here we show in experimental models and in patients that loss of *IKZF1* promotes resistance to cytarabine (AraC), a key component of both upfront and relapsed treatment protocols. We attribute this resistance, in part, to diminished import and incorporation of AraC due to reduced expression of the solute carrier hENT1. Moreover, we found elevated mRNA expression of Evi1, a known driver of therapy resistance in myeloid malignancies. Finally, a kinase directed CRISPR/Cas9-screen identified that inhibition of either mediator kinases CDK8/19 or casein kinase 2 can restore response to AraC. We conclude that this high-risk group of patients could benefit from alternative antimetabolites, or targeted therapies that re-sensitize leukemic cells to AraC.

Introduction

With contemporary treatment protocols, close to 95% of all pediatric B-cell precursor acute lymphoblastic leukemia (BCP-ALL) patients are cured.¹ However, about 10% of pediatric BCP-ALL patients still experience relapsed disease.¹ Moreover, the intense multi-agent chemotherapy regimens used for the treatment of BCP-ALL come with many acute and long-term side-effects as well as treatment-related mortality.² While reduced intensity treatment for patients with favorable genetic profiles has been successfully introduced,³ options remain limited for high-risk leukemia subtypes, as the dose intensity of conventional chemotherapy has been pushed to its limit. This underscores the need for alternative more effective treatment strategies for high-risk BCP-ALL, which take into account leukemia-specific drug sensitivity profiles.² Deletions or mutations affecting the lymphoid tran-

scription factor *IKZF1* occur in approximately 10-15% of pediatric BCP-ALL patients and are associated with poor outcome.⁴⁻⁶ In about 80% of the *IKZF1*-deleted relapses, the *IKZF1*-deleted clone was preserved from diagnosis, suggesting that loss of *IKZF1* function contributes to therapy resistance.⁷ Loss of *IKZF1* function promotes cell-intrinsic resistance to synthetic glucocorticoids,^{6,8} which can be reversed by the use of small molecule inhibitors.⁹ To what extent loss of *IKZF1* function affects sensitivity to other drugs used in contemporary treatment protocols has not been explored.

Here, we modeled loss of *IKZF1* function in BCP-ALL cell lines and patient-derived xenografts (PDX) and compared cellular responses to various chemotherapeutic agents used in the treatment of BCP-ALL. We demonstrated that loss of *IKZF1* function is associated with resistance to cytarabine (AraC) and we investigated the underlying mechanisms.

Methods

Detailed descriptions of the experiments can be found in the *Online Supplementary Methods*.

Ethical statement

PDX were generated from patients' samples collected from different countries within International BFM Study Group (I-BFM-SG) and Dutch Childhood Oncology Group (DCOG) studies. All patients were enrolled in trials on treatment of pediatric BCP-ALL conducted by individual member groups of the I-BFM-SG: the AIEOP-BFM study group (Austria, Germany, Italy and Switzerland), the FRALLE study group (France) and the United Kingdom (UK) National Cancer Research Institute (NCRI) Childhood Cancer and Leukemia Group and the DCOG. All treatment trials were approved by the respective national institutional review boards, and informed consent for the use of spare specimens for research was obtained from study individuals, parents, or legal guardians.

Real-time quantitative polymerase chain reaction-based minimal residual disease analyses

Minimal residual disease (MRD) levels of patients treated within the ALL-10 or ALL-11 treatment protocol were routinely determined by real-time quantitative polymerase chain reaction (RT-qPCR) analysis of immunoglobulin (IG) and/or T-cell receptor (TR) gene rearrangements, and the laboratory participated in the quality control rounds of the EuroMRD network (see www.EuroMRD.org). RT-qPCR data, acquired in triplicate, were analyzed according to EuroMRD guidelines, applying criteria to prevent false-negative MRD results.¹⁰ To calculate the log reduction between time point 1 (TP1, day 33) and time point 2 (TP2, day 79), patients with MRD levels $\geq 10^{-2}$ at TP1 were selected (providing 2 log steps for quantitative analysis). To allow calculations of log reduction, positive non-quantifiable MRD data ($< 10^{-4}$) were arbitrarily set at a value of 5×10^{-5} and negative MRD data were set at 1×10^{-6} . All MRD values were 10log-transformed, and the resulting values of TP2 were divided by those from TP1.

In vivo mouse trial

This study followed international, national, and/or institutional guidelines for humane animal treatment and complied with relevant legislation. Ethical approval was obtained from the Animal Experimental Committee of Radboud University (RU-DEC-2019-0036). *IKZF1* mutated and wild-type BCP-ALL xenografts were intravenously injected, with 1×10^6 viable cells in two mice per patient sample. One mouse of each pair was treated with AraC for 2 weeks (5 days on, 2 days off) and the delay in leukemia formation was calculated as described in the *Online Supplementary Methods*.

CRISPR/Cas9 screen

For this CRISPR/Cas9 screen, cells were exposed to 30 nM and 50 nM AraC for 22 days, all in triplicate. Cells were se-

quenced and enriched and depleted genes were identified using the MAGeCK Test algorithm (Galaxy Version 0.5.8.1) (*Online Supplementary Table S2*).

Statistical analyses

P values were considered statistically significant when < 0.05 and are illustrated as following * $P < 0.05$, ** $P < 0.01$, *** $P < 0.001$, **** $P < 0.0001$.

Results

Loss of *IKZF1* protects against cytarabine-induced apoptosis

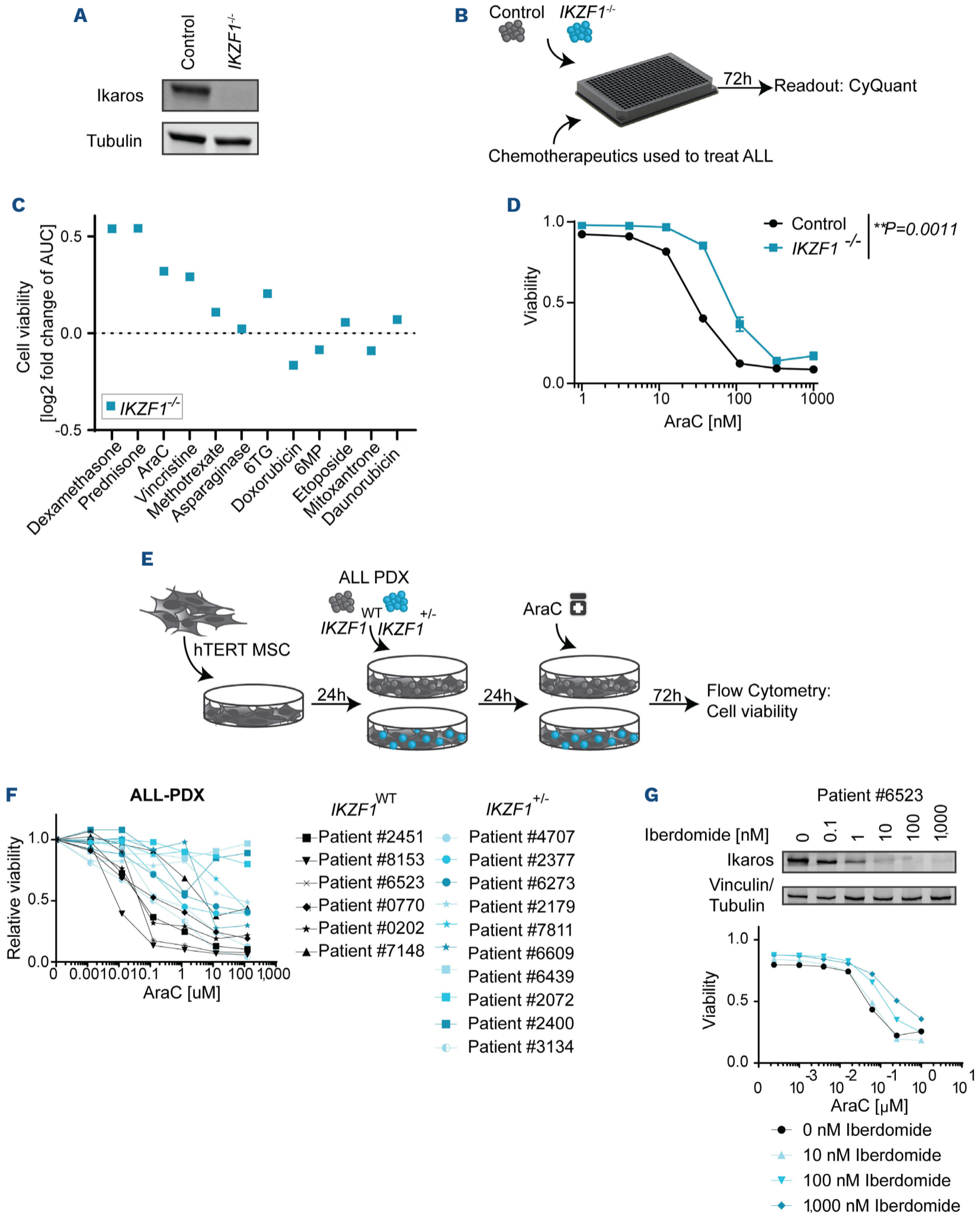
To investigate the potential effects of *IKZF1* loss of function on cellular drug responses, we performed a drug screen in the BCP-ALL cell line Sem where we modeled *IKZF1* loss of function. As demonstrated earlier,⁹ a bi-allelic CRISPR/Cas9-induced frameshift mutation resulted in a complete loss of protein expression (Figure 1A) which, unlike a heterozygous mutation, led to a stable genotype. No difference in cell growth was observed between *IKZF1*^{-/-} and control cells (*Online Supplementary Figure S1A*), indicating that drug responses are not a consequence of a lower proliferation rate. These *IKZF1* knockout cells were exposed to a panel of drugs used in the treatment of BCP-ALL and sensitivity was determined by measuring cell numbers using CyQuant dye and compared to that of control cells transduced with non-targeting gRNA (Figure 1B). In addition to the expected resistance to the glucocorticoids prednisolone and dexamethasone, *IKZF1*^{-/-} cells displayed a reduced response to two other drugs in the treatment protocol, AraC and vincristine (Figure 1C, *Online Supplementary Figure S1B*). We repeated this assay using a more specific cell death measurement by testing for membrane integrity using flow cytometric detection of the binding of amine reactive dyes. This assay confirmed a diminished efficacy of the nucleoside analog AraC in addition to glucocorticoid resistance in this model (Figure 1D), while no effect on the response to vincristine was seen (*data not shown*). In addition to amine exposure, DNA fragmentation and PARP cleavage assays confirmed increased resistance to AraC treatment for *IKZF1*^{-/-} cells (*Online Supplementary Figure S2A, B*).

Endogenous *IKZF1* gene deletions as well as pharmacological targeting of Ikaros protein in B-cell precursor acute lymphoblastic leukemia xenografts correlate with resistance against AraC *ex vivo* and *in vivo*

To validate our results in models that more closely reflect primary BCP-ALL, we compared the response to AraC in a panel of PDX, cultured on feeder layers of immortalized bone marrow stroma cells.¹¹ First, we tested to what extent endogenous gene deletions of *IKZF1* affect response to AraC treatment (Figure 1E). A panel of 16 BCP-ALL PDX, each derived from samples obtained at diagnosis, being either

wild-type for *IKZF1* (N=6) or carrying clonal *IKZF1* deletions (N=10), were incubated with increasing concentrations of AraC. After 3 days, cell viability was measured by staining with amine reactive dyes and quantified by flow cytometry. Data were plotted as dose-response curves (Figure

1F) and the area under the curve (*Online Supplementary Figure S2C*) was calculated as a measure of sensitivity. Similar to our findings in the model cell line, *IKZF1*-deleted PDX showed significantly increased resistance to AraC compared to PDX wild-type for *IKZF1*. In addition,



Continued on following page.

Figure 1. Deletion of *IKZF1* drives resistance to AraC *in vitro*. (A) Immunoblot analysis of *IKZF1* protein expression in single cell clones upon CRISPR/Cas9-based targeting of *IKZF1*. Representative blot of three independent experiments. (B) Schematic overview representing the workflow used to determine drug responses. Sem wild-type (WT) and Sem *IKZF1*-deleted (*IKZF1*^{-/-}) cells were seeded into 384-well plates and treated with drugs used in contemporary treatment protocols for pediatric B-cell precursor acute lymphoblastic leukemia (BCP-ALL) patients. After 3 days of incubation, cell death was analyzed by fluorescence intensity using the live cell staining CyQuant. (C) Fold change in cell viability relative to cells wild-type for *IKZF1* upon drug exposure. Corresponding dose response curves can be found in *Online Supplementary Figure S1*. (D) Cytarabine (AraC)-induced cell death as determined by quantification of cells positive for amine-reactive dyes using flow cytometry in Sem WT and Sem *IKZF1*^{-/-} cells after 3 days of treatment with increasing concentrations of AraC (mean ± standard error of the mean [SEM], N=3, **P=0.0011, two-sided *t* test based on area under curve values). (E) Schematic overview representing the workflow used to determine *ex-vivo* drug responses in patient-derived xenograft (PDX) samples. BCP-ALL PDX, either WT or carrying a heterozygous clonal deletion of *IKZF1* (*IKZF1*^{+/-}), were seeded on hTERT immortalized mesenchymal stem cells, allowed to settle for 24 hr and then treated with increasing concentrations of AraC. After 3 days of incubation cell death was determined by quantification of cells positive for amine-reactive dyes using flow cytometry. (F) Cell viability determined by amine staining in PDX either WT (black, n=6) or *IKZF1*^{+/-} (blue, n=10) as dose response curves. Of note, the least responsive WT sample, Patient #7148, harbors a t(17::19), a chromosomal translocation known to induce multiagent drug resistance; such patients have an extremely poor prognosis. (G) Representative PDX sample for pharmacological targeting of the Ikaros protein using Iberdomide. Immunoblot analysis of *IKZF1* protein expression showing degradation of *IKZF1* protein in response to Iberdomide treatment after 24 hours, in different PDX samples. AraC induced cell death was determined by quantification of cells positive for amine-reactive dyes using flow cytometry after 3 days of treatment with increasing concentrations of AraC in the presence or absence of the indicated doses of iberdomide. Results for other tested PDX samples (N=6) can be found in *Online Supplementary Figure S2D*. ALL: acute lymphoblastic leukemia; AUC: area under the curve; 6TG: 6-thioguanine; MSC: mesenchymal stem cells.

we studied the effect of pharmacological modulation of *IKZF1* protein levels in PDX samples wild-type for *IKZF1* to rule out differences in genetic background and looked at an isolated effect of *IKZF1* loss. For this, we used thalidomides, a class of immunomodulatory agents that act by targeting the lymphoid transcription factors *IKZF1* and *IKZF3* for proteasome-mediated degradation by the Cul4A^{CRBN} E3 ligase complex.¹² These agents are used in the treatment of multiple myeloma and myeloid neoplasms such as myelodysplastic syndrome. We selected iberdomide, a highly *IKZF1*-specific thalidomide in this class,¹³ and tested therapy response to AraC in seven BCP-ALL PDX models wild-type for *IKZF1* (Figure 1G, *Online Supplementary Figure S2D*). Indeed, 24-hour exposure to >10 nM iberdomide led to effective degradation of *IKZF1* protein expression in these PDX and induced resistance to AraC in six out of seven tested PDX (Figure 1G, *Online Supplementary Figure S2D*). In the one xenograft (Patient #3862) that showed no significant effect of iberdomide treatment on AraC therapy response, iberdomide-mediated *IKZF1* degradation appeared to be less effective (*Online Supplementary Figure S2D*).

To show that the *ex vivo* response to therapeutic drugs accurately reflects the sensitivity to *in vivo* treatment, we performed a mouse trial (Figure 2A). This experimental setup allows for a greater number of leukemia models to be tested at the same time, enabling better representation of the disease subtype.¹⁴ We selected a panel of ten PDX (4 wild-type for *IKZF1* and 6 *IKZF1*^{+/-}) and injected each into two mice. Upon overt signs of leukemia, as measured by the presence of at least 1% of human cells in the blood (*Online Supplementary Figure S3A*), one mouse of each pair was treated with AraC and leukemia development was compared to that in its untreated counterpart. By comparing the treatment-induced delay in leukemia de-

velopment, we established that *IKZF1*-deleted PDX samples are less affected by AraC treatment *in vivo* (Figure 2B). Of note, the PDX samples that were most resistant *ex vivo* were also least affected by AraC treatment *in vivo*, highlighting the predictive value of *ex vivo* drug response profiling of patient-derived cells in co-culture systems (Figures 1F and 2B; *Online Supplementary Figure S3B*). In PDX samples tested both *ex vivo* and *in vivo* we found increased resistance towards AraC in samples harboring an *IKZF1* deletion, similar to our cell line model.

B-cell precursor acute lymphoblastic leukemia patients with *IKZF1* gene alterations show a reduced response to an AraC-containing consolidation block

In contrast to our previous study in which the response to glucocorticoids could be evaluated during a week-long single-agent treatment,⁸ current protocols dictate the use of AraC in a combination with other drugs. This complicates the assessment of the relative contribution of AraC. During the first consolidation phase of the recent Dutch ALL-10 and ALL-11 treatment protocols for pediatric BCP-ALL, patients are for the first time exposed to AraC, where they receive a cumulative dose of 1,200 mg/m² AraC.^{3,15} Of note, in contemporary relapsed ALL protocols, higher doses of AraC are used. The consolidation block also contains 6-mercaptopurine 60 mg/m²/day p.o. for 28 days and two doses of 1,000 mg/m² cyclophosphamide.^{3,16} Patients also received one or two doses of PEG-asparaginase and/or received two doses of intrathecal triple therapy (methotrexate, AraC and prednisolone at age-adjusted dosages) during this period. As this treatment block is flanked by MRD measurements we were able to assess the effects of treatment on leukemia burden (Figure 2C). Since loss of *IKZF1* reduces response to synthetic glucocorticoids,⁸ patients with *IKZF1*-deleted leukemias show elevated MRD

levels at the end of induction. To obtain a quantifiable MRD range for our comparison, we selected all patients with high MRD after induction at TP1, as described in the Methods section. Because of this selection, MRD levels

between *IKZF1*-deleted and *IKZF1* wild-type BCP-ALL patients at the start of the AraC-containing treatment block did not differ (Figure 2D). To assess the potential effect of *IKZF1* deletions during consolidation, we analyzed the

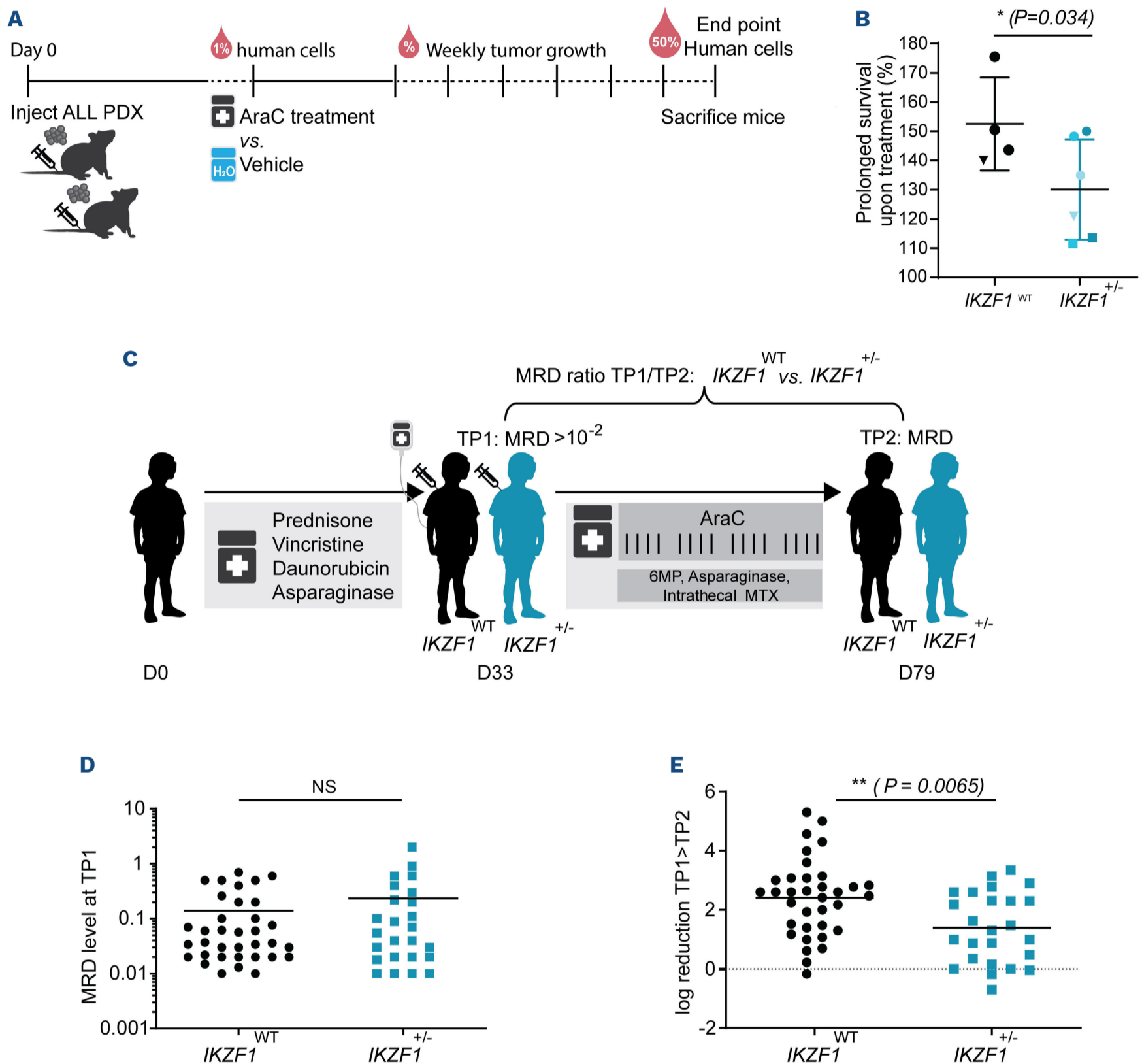


Figure 2. *IKZF1*-deleted leukemias show resistance to AraC *in vivo*. (A) Timeline of the *in vivo* mouse trial. Each B-cell precursor acute lymphoblastic leukemia (BCP-ALL) patient-derived xenograft (PDX) was injected into two mice at day 0 and leukemia growth was measured weekly by flow cytometry. At 1% of human cells in the blood, mice were treated twice for 5 days with a break of 2 days in between, one of the pair receiving cytarabine (AraC) and the other vehicle. Leukemia growth was tracked weekly by flow cytometry and mice were sacrificed when there were >50% human cells in the blood. (B) *In vivo* delay of leukemia growth upon AraC treatment in PDX wildtype (WT) for *IKZF1* and samples with heterozygous clonal deletion of *IKZF1* (*IKZF1*^{+/-}) (mean ± standard error of the mean, **P*=0.034, two-sided *t* test). (C) Schematic overview representing the workflow used to determine minimal residual disease (MRD) response in BCP-ALL patients in relation to *IKZF1*. Cases were selected that showed MRD levels >10⁻² at timepoint 1 (TP1, day 33) and the response at timepoint 2 (TP2, day 79) was followed. (D) MRD levels at TP1 of patients WT for *IKZF1* (N=35) or patients carrying a heterozygous deletion of *IKZF1* (N=25). *P*=0.7867, Mann-Whitney, two-tailed test. (E) Ratio of MRD between TP1 and TP2 log₁₀-transformed (TP1>TP2) of patients WT for *IKZF1* or carrying a heterozygous deletion of *IKZF1* after receiving a therapy block including AraC and 6-mercaptopurine ***P*=0.0065, Mann-Whitney, two-tailed test. 6-MP: 6-mercaptopurine; MTX: methotrexate; NS: not statistically significant.

reduction of leukemia burden in MRD from TP1 (day 33) to TP2 (day 79). We observed that the fold reduction of MRD levels after the AraC-containing therapy block was significantly less for *IKZF1*-deleted patients compared to *IKZF1* wild-type patients, indicating increased treatment resistance in the former patients (Figure 2E). Although we cannot exclude that reduced sensitivity to 6-mercaptopurine or other drugs may have contributed to these effects, we did not observe such a diminished response to asparaginase or 6-mercaptopurine in our *in vitro* assays (Figure 1C). We therefore attribute the observed reduced response to resistance to AraC in these *IKZF1*-deleted BCP-ALL patients

Decreased hENT1 expression contributes to AraC resistance induced by *IKZF1* loss

Most nucleoside analogs require active import and anabolic processing before the biologically active compound becomes available. This requirement poses a weakness that can be exploited by leukemia cells for the development of resistance (*Online Supplementary Figure S4A*). Resistance to nucleoside analogs can be a consequence of ineffective cellular uptake, for instance due to reduced expression of nucleoside transporters, or changes in metabolic handling of these drugs.¹⁷ On the other hand, failed execution of apoptosis has also been reported in, for example, P53 null cells.¹⁸ To identify which of these mechanisms contributes to the resistance phenotype of *IKZF1*-deleted cells, we used mass spectrometry to measure the incorporation of the active compound AraCTP in *IKZF1*^{-/-} cells versus control Sem cells (Figure 3A). This showed a marked reduction of AraCTP incorporation into *IKZF1*-deleted cells. Previous studies have identified several proteins contributing to AraC incorporation into the DNA in acute myeloid leukemia (AML) (hENT1, dCK, CDA, 5NT, TOPO I, TOPO II, DNA POL and MDR1).^{17,19} To test whether any of these proteins contributed to *IKZF1*-mediated AraC-resistance, we analyzed the relative expression of the genes encoding these proteins in *IKZF1*^{-/-} cells relative to control Sem cells (Figure 3B). Only hENT1, the solute carrier that transports AraC over the cell membrane (*Online Supplementary Figure S4A*), showed decreased mRNA expression in *IKZF1*^{-/-} cells, which also translated into decreased protein expression (Figure 3C-E). Indeed, overexpression of hENT1 in *IKZF1*^{-/-} cells could sensitize cells to AraC treatment again (*Online Supplementary Figure S4B*). In addition, iberdomide-mediated *IKZF1* degradation correlated with decreased hENT1 mRNA expression in four tested PDX (Figure 3F). A trend towards lower hENT1 expression was also visible when we compared RNA-sequencing data from primary patient material obtained at diagnosis (Figure 3G). Particularly in the B-other group, the subset that contains the majority of *IKZF1*-deleted leukemias, lower hENT1 expression was seen in *IKZF1*-deficient samples, although the number of patients was too small for the statistical threshold to

be reached (*Online Supplementary Figure S4C*). Together our experiments indicate that loss of hENT1 expression contributes to *IKZF1*-driven AraC therapy resistance.

Loss of *IKZF1* promotes expression of the Evi1 oncogene

To obtain deeper insights into pathways or specific genes driving resistance to AraC upon loss of *IKZF1*, we performed RNA sequencing on samples from wild-type and *IKZF1* knockout Sem cells treated or not with AraC. We compiled a list of differentially expressed genes in response to treatment or as result of *IKZF1* loss (Figure 4A) and determined which KEGG pathways are overrepresented in this selection (Figure 4B, *Online Supplementary Figure S5A*). Three of the highest scoring pathways, focal adhesion, PI3K-AKT and MAPK, have previously been implicated in *IKZF1*-mediated resistance to kinase inhibitor and glucocorticoid treatment.^{9,20} Indeed, modulation of these pathways using the AKT inhibitor MK2206, the ERK inhibitor uprosertib or their combination enhanced the response to AraC, similarly to what we have shown for prednisolone-induced apoptosis⁹ (Figure 4C). This corroboration of previous findings further strengthens the validity of our loss-of-function model. Since *IKZF1* functions as a repressive transcription factor, we focused on upregulated genes and pathways. *MECOM*, a gene annotated as a component of the MAPK pathway (Figure 4D), caught our attention as it is frequently overexpressed in AML, in which it dictates a poor outcome. *MECOM* encodes the zinc finger transcription factor Evi1, a prominent oncogene mostly known for its role in the pathogenesis of AML and chronic myeloid leukemia,²¹ yet undefined in BCP-ALL. Evi1 is essential for the maintenance of a stemness phenotype in hematopoietic stem cells.²² Several studies implicate Evi1 in AraC resistance in AML, suggesting a similar role for Evi1 in inducing resistance in BCP-ALL.^{23,24} We used RT-qPCR to confirm that loss of *IKZF1* promotes expression of Evi1 in Sem cells and we observed that expression was further induced in response to AraC treatment (Figure 4E). A similar response was found in four out of five tested PDX samples, where both iberdomide-induced *IKZF1* degradation and AraC treatment promoted Evi1 expression (Figure 4F). Only in patient sample #3862, in which iberdomide failed to effectively induce *IKZF1* degradation and AraC resistance (*Online Supplementary Figure S2D*), did Evi1 expression also not elevate. Although Evi1 expression increased by 15-fold when *IKZF1*-deleted Sem cells were treated with AraC, this expression is still ~50 fold lower than that of AML cells carrying the t(3::8)(q26::q24) translocation, the genetic event that most commonly results in upregulation of Evi1 in AML patients (*Online Supplementary Figure S5B,C*). Although we were unable to detect Evi1 protein expression in our *IKZF1*-knockout cells, these cells did not tolerate modulation of Evi1 protein levels as after shRNA-mediated knockdown using four different shRNA, these cells were rapidly lost from the culture within 2 days, while

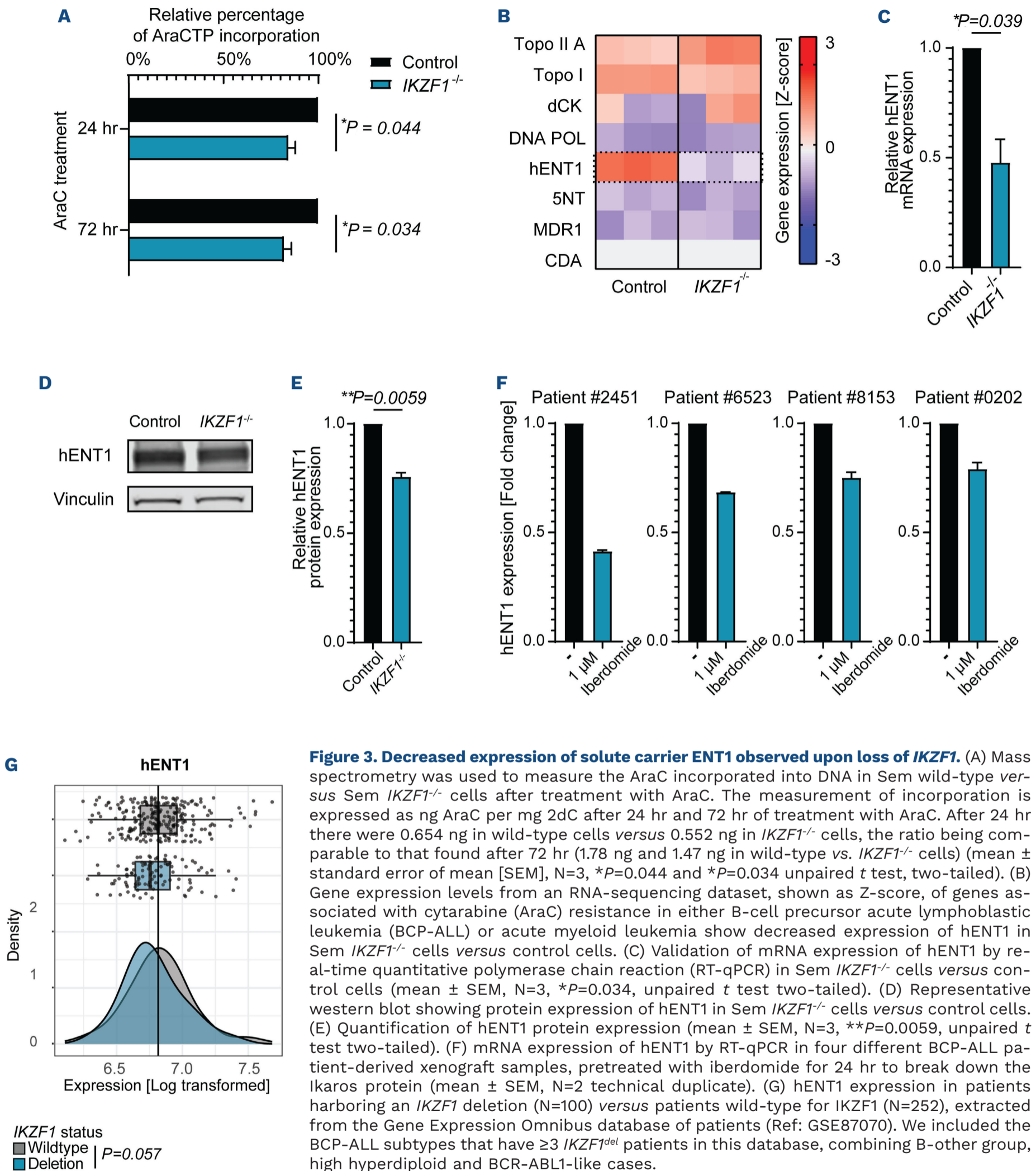
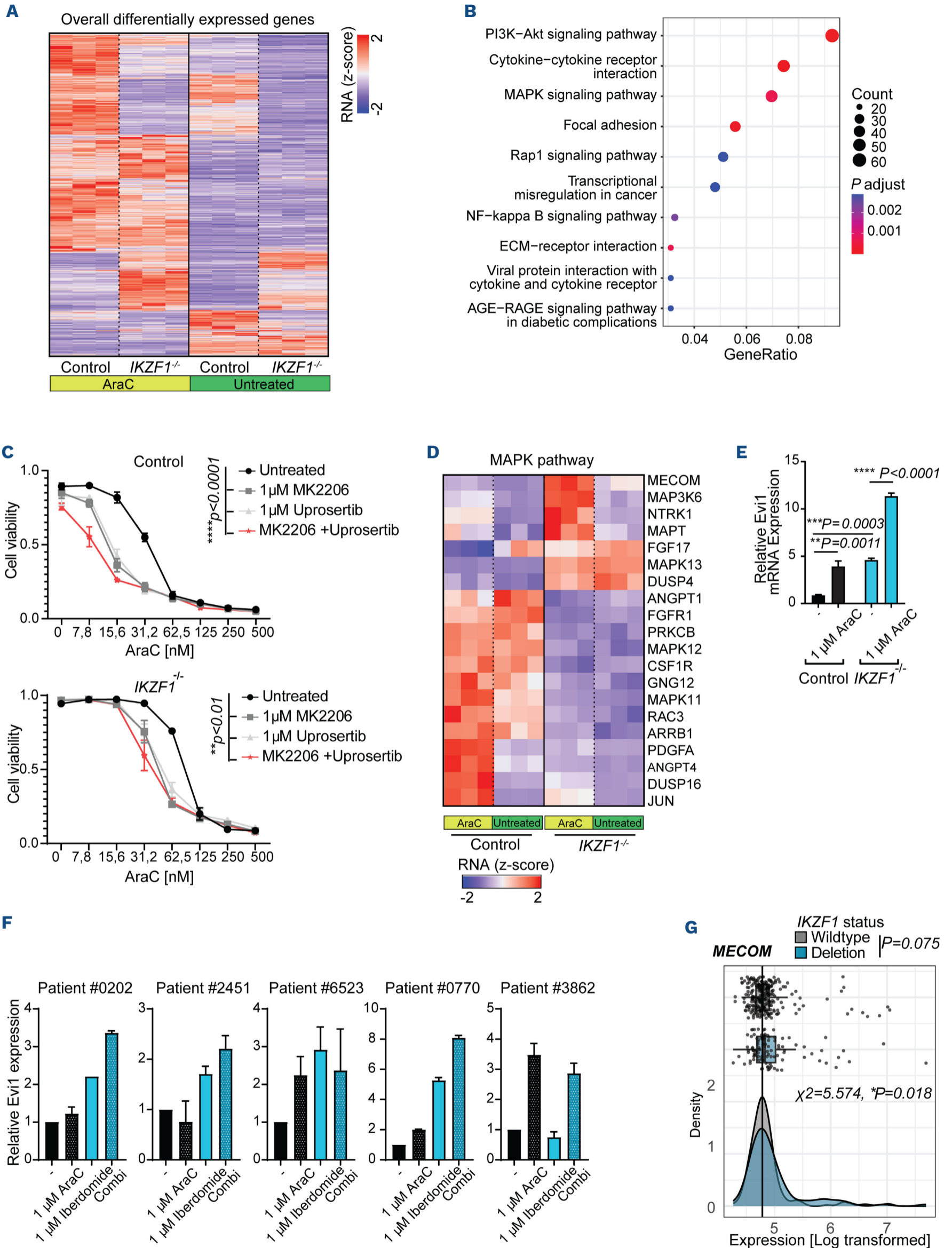


Figure 3. Decreased expression of solute carrier ENT1 observed upon loss of *IKZF1*. (A) Mass spectrometry was used to measure the AraC incorporated into DNA in Sem wild-type versus Sem *IKZF1*^{-/-} cells after treatment with AraC. The measurement of incorporation is expressed as ng AraC per mg 2dC after 24 hr and 72 hr of treatment with AraC. After 24 hr there were 0.654 ng in wild-type cells versus 0.552 ng in *IKZF1*^{-/-} cells, the ratio being comparable to that found after 72 hr (1.78 ng and 1.47 ng in wild-type vs. *IKZF1*^{-/-} cells) (mean ± standard error of mean [SEM], N=3, *P=0.044 and *P=0.034 unpaired *t* test, two-tailed). (B) Gene expression levels from an RNA-sequencing dataset, shown as Z-score, of genes associated with cytarabine (AraC) resistance in either B-cell precursor acute lymphoblastic leukemia (BCP-ALL) or acute myeloid leukemia show decreased expression of hENT1 in Sem *IKZF1*^{-/-} cells versus control cells. (C) Validation of mRNA expression of hENT1 by real-time quantitative polymerase chain reaction (RT-qPCR) in Sem *IKZF1*^{-/-} cells versus control cells (mean ± SEM, N=3, *P=0.034, unpaired *t* test two-tailed). (D) Representative western blot showing protein expression of hENT1 in Sem *IKZF1*^{-/-} cells versus control cells. (E) Quantification of hENT1 protein expression (mean ± SEM, N=3, **P=0.0059, unpaired *t* test two-tailed). (F) mRNA expression of hENT1 by RT-qPCR in four different BCP-ALL patient-derived xenograft samples, pretreated with iberdomide for 24 hr to break down the Ikaros protein (mean ± SEM, N=2 technical duplicate). (G) hENT1 expression in patients harboring an *IKZF1* deletion (N=100) versus patients wild-type for *IKZF1* (N=252), extracted from the Gene Expression Omnibus database of patients (Ref: GSE87070). We included the BCP-ALL subtypes that have ≥3 *IKZF1*^{del} patients in this database, combining B-other group, high hyperdiploid and BCR-ABL1-like cases.

control cells continued to proliferate. This suggests that, albeit expressed at low levels, Evi1 is essential for these *IKZF1* knockout cells to survive. Similar to what has been observed for AML cells,²⁵ forced expression of Evi1 from

a retrovirus also resulted in immediate cell cycle arrest in our BCP-ALL models, while control cells continued to proliferate (*data not shown*). Of note, although we did not observe significant differences of Evi1 expression



Continued on following page.

Figure 4. Gene expression changes in the MAPK pathway reveal upregulated expression of Evi1 (*MECOM*) in *IKZF1*^{-/-} cells. (A) Compiled heatmap created by unsupervised clustering of genes differentially expressed in response to cytarabine (AraC) treatment or as a result of *IKZF1* loss from bulk RNA-sequencing data on Sem *IKZF1*^{-/-} and control cells. Cells were treated with 1 mM AraC for 16 hr and samples were harvested in triplicate. (B) KEGG pathway overrepresentation analysis was performed on the compiled list of differentially expressed genes from (A), with the ten highest scoring pathways shown here. (C) Cell viability determined in Sem *IKZF1*^{+/-} and control cells by amine staining as dose-response curves for AraC treatment in combination with the AKT inhibitor MK2206 and the ERK inhibitor uposertib (mean ± standard error of mean [SEM], N=3, **P=0.0011, analysis of variance [ANOVA] followed by the Tukey multiple comparisons test). (D) Heatmap created by unsupervised clustering of the MAPK pathway, only showing genes differentially expressed between control and *IKZF1*^{-/-} cells upon AraC treatment. The heatmap was created using the FPKM (fragments per kilobase of transcript per million mapped reads) values transformed into Z-scores. (E) Validation of Evi1 (*MECOM*) mRNA expression by real-time quantitative polymerase chain reaction (RT-qPCR) in Sem *IKZF1*^{-/-} cells versus control cells upon treatment with 1 mM AraC for 16 hr (mean ± SEM, N=3, ANOVA followed by the Tukey multiple comparisons test). (F) mRNA expression of *MECOM* by RT-qPCR in five different B-cell precursor acute lymphoblastic leukemia (BCP-ALL) patient-derived xenograft samples, pretreated with iberdomide for 24 hr (mean ± SEM, N=2 technical duplicate). (G) *MECOM* expression in patients harboring an *IKZF1* deletion (N=100) versus patients wild-type for *IKZF1* (N=352), extracted from the Gene Expression Omnibus database (GSE87070). Here we included those BCP-ALL subtypes that had ≥3 *IKZF1*^{del} patients in this database, combining here the B-other, BCR-ABL1-like and high hyperdiploid subgroups. A χ^2 test was performed to calculate the correlation between *IKZF1* mutations and elevated Evi1 expression ($\chi^2=5.574$, *P=0.018).

in RNA-sequencing data from primary patient material, leukemias harboring *IKZF1* deletions were more likely to show high Evi1 expression, as defined by a χ^2 test, compared to those wild-type for *IKZF1* ($\chi^2=5.574$, *P=0.018) (Figure 4G, *Online Supplementary Figure S5D*). Similar to AML, BCP-ALL samples expressing high Evi1 levels showed increased mRNA expression of stem cell markers (*Online Supplementary Figure S5E*). Although the correlation between *IKZF1* mutations and elevated Evi1 expression may be dependent on co-occurring events, our data indicate that *IKZF1* loss can result in increased expression of Evi1 which, at least in a subset of leukemias, may contribute to a poor response to therapy.

Inhibition of mediator kinases CDK8/19 or casein kinase II sensitizes the response to AraC

In search of druggable targets that could reverse AraC therapy resistance in *IKZF1*-deleted ALL, we performed a CRISPR/Cas9-based loss-of-function screen with a sgRNA library targeting all human kinases (N=507) in Sem *IKZF1*^{-/-} cells (Figure 5A). We performed two independent screens using low doses of AraC (30 nM and 50 nM) for 3 weeks allowing selection of enriched or depleted sgRNA (*Online Supplementary Figure S6A, B*). Using the MaGeCK algorithm,²⁶ sgRNA counts between treated and untreated cells were compared. Of note, both screening conditions showed a substantial overlap in the top ranked depleted and enriched genes, emphasizing the accuracy and reproducibility of this approach (Figure 5B, *Online Supplementary Figure S6C, Online Supplementary Table S2*).

We focused on depleted sgRNA (dropouts), as loss of function of their target genes can be expected to enhance response to AraC. As expected, we found Akt1 as an enhancer of AraC response within the top 20 depleted genes for both screening conditions (*Online Supplementary Table S2*), which confirms our earlier findings (Figure 4C). Among the highest scoring depleted genes in both screens, we identified the homologous cyclin dependent kinases

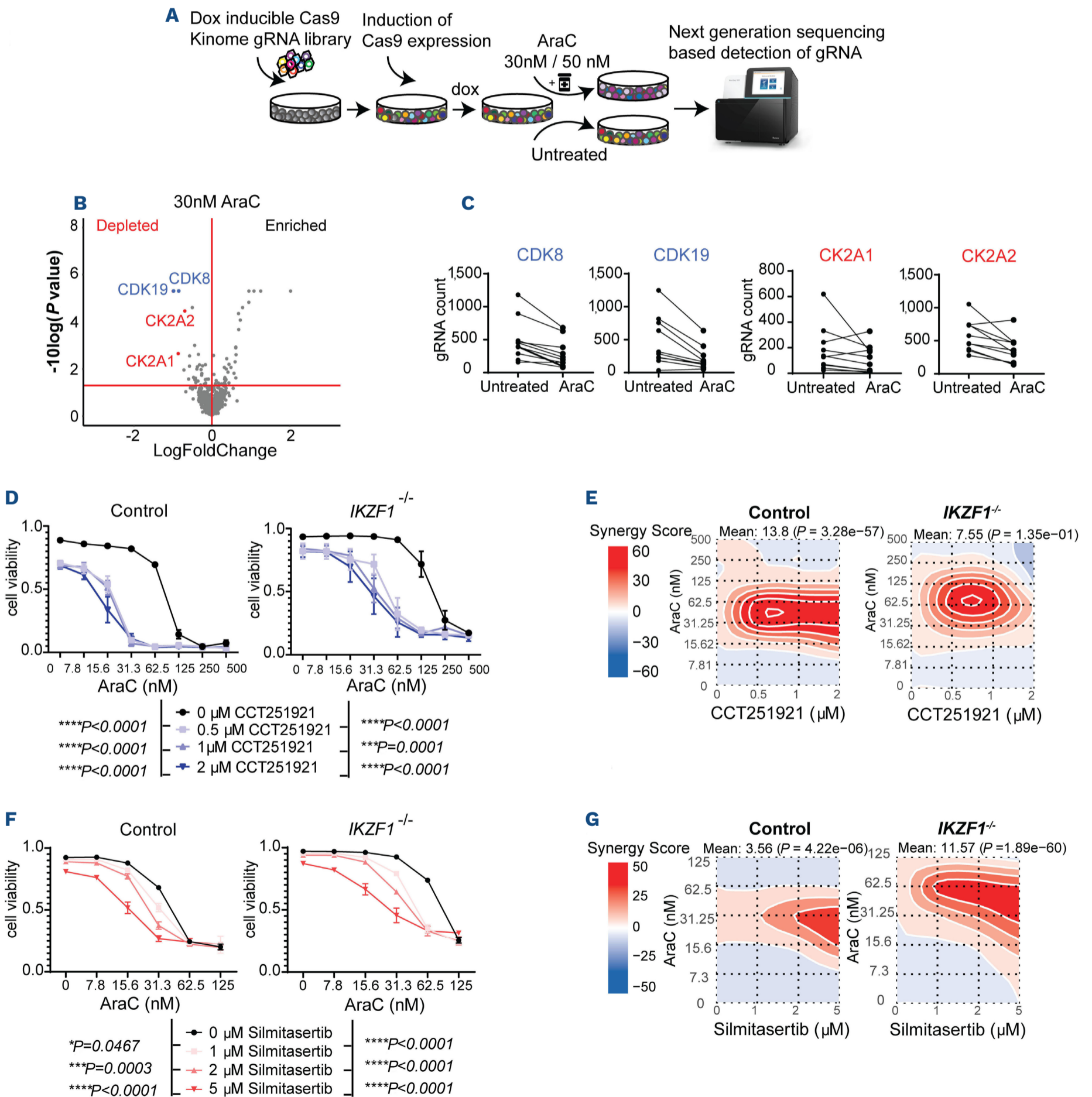
CDK8/19. These mediator kinases regulate transcriptional programming and the metabolic homeostasis of cells and CDK8/19 inhibitors have been shown to prevent the development of resistance to different classes of drugs.²⁷ To validate these targets, we used the small molecule inhibitor CCT251921, specifically targeting CDK8 and 19, at concentrations that marginally affect cell viability as a single agent, but in combination with AraC strongly synergized in both Sem wild-type and *IKZF1*^{-/-} cells by decreasing half maximal inhibitory concentration (IC₅₀) values ~5.2-fold at the highest concentration of the inhibitor (Figure 5D, E, *Online Supplementary Figure S6D*). Therefore, this combination therapy appears to enhance therapy response to AraC, independently of *IKZF1* status. In addition, we identified the sgRNA targeting *CK2A1* and *CK2A2* among the strongest depleted genes in both screens (Figure 5B, *Online Supplementary Figure S6C*). *CK2* encodes casein kinase II (CK2) and plays a prominent role in promoting cell growth, suppression of apoptosis and drug resistance in solid and hematologic malignancies.²⁸ More importantly, growing evidence shows that CK2 directly regulates transcription factor *IKZF1*.²⁹ In the case of hemizygous *IKZF1* deletions in leukemia, inhibition of CK2 can restore the function of the intact *IKZF1* allele.³⁰ It is therefore an interesting, although unexpected, hit in our CRISPR/Cas9 screen since the Sem *IKZF1*^{-/-} cell line model has no intact allele left to restore, suggesting additional mechanisms are taking place. It was shown that CK2 also phosphorylates Evi1 to enhance its activity, providing a potential explanation for the observed phenotype.³¹ As a validation of our CRISPR/Cas9 screen, we established that the CK2 inhibitor silmitasertib synergized with AraC in both Sem wild-type cells and *IKZF1*^{-/-} cells, although the highest synergy was observed in *IKZF1*-deficient cells (IC₅₀ decrease of ~2.3 fold in wild-type vs. ~3.5 fold in *IKZF1*^{-/-} cells), (Figure 5F, *Online Supplementary Figure S6E*). These findings indicate that inhibition of CK2, a modulator of both Evi1 and *IKZF1* activity, may offset the effects of

IKZF1 loss on AraC therapy resistance.

Discussion

In this study we used genetic and pharmacological targeting of *IKZF1* to show that loss of *IKZF1* function reduces the response to AraC, a component of both upfront and relapsed BCP-ALL treatment protocols. This observation

contrasts with an earlier observation suggesting that *IKZF1* loss induces sensitivity to this nucleoside analog.³² However, our findings are corroborated by *in vitro* and *in vivo* studies using PDX and a retrospective analysis of MRD in patients. The insensitivity of *IKZF1*-deleted cells may, at least in part, be the result of reduced AraCTP incorporation (Figure 3A), a causality that was established already decades ago.³³ We attribute this diminished incorporation to a reduced availability of intracellular AraC because of



Continued on following page.

Figure 5. CRISPR/Cas9 kinome screen revealed targetable genes to sensitize cells to AraC treatment. (A) Schematic representation of our CRISPR screening strategy. Sem *IKZF1*^{-/-} cells were transduced with a kinome sgRNA library and cultured for 2 weeks in the presence of 1 mg/mL doxycyclin to induce Cas9 expression. Cells were then split into three pools and treated for 22 days with either 0 nM, 30 nM or 50 nM cytarabine (AraC). DNA was isolated and subjected to Illumina next-generation sequencing. (B) Volcano-plot of sgRNA targets that significantly modulate response to AraC, based on *P* value and log-fold change as analyzed using the MaGeCK test algorithm. The top depleted genes overlap between the 30 nM and 50 nM AraC (*Online Supplementary Figure S6C*) screens, as marked in red. (C) Counts of individual sgRNA targeting CDK8, CDK19, CK2A1 and CK2A2 between the untreated cells and cells treated with 30 nM AraC after screening for 22 days. (D) Combination therapy-induced cell death as determined by quantification of cells positive for amine-reactive dyes using flow cytometry in Sem control and Sem *IKZF1*^{-/-} cells after 5 days of treatment with increasing concentrations of AraC and the CDK8/19 inhibitor CCT251921. Each data point represents a mean (\pm standard error of mean [SEM]) of three independent experiments. Two-way analysis of variance (ANOVA) was performed on the area under the curve (AUC) values of the inhibitor in combination with AraC versus AraC as a single treatment, for both genotypes ($***P < 0.001$, $****P < 0.0001$). Absolute half-maximal inhibitory concentration (IC_{50}) values in wild-type cells were 80.8 nM for AraC only versus 14.9 nM in combination with 2 mM CCT251921 and 155.8 nM for only AraC and 30.9 nM for the combination in *IKZF1*^{-/-} cells. (E) Synergy scores generated by Synergy finder software, using the values from Figure 5D. (F) Combination therapy-induced cell death as determined by quantification of cells positive for amine-reactive dyes using flow cytometry in Sem control and Sem *IKZF1*^{-/-} cells after 5 days of treatment with increasing concentrations of AraC and the CK2 inhibitor sil-mita-sertib. Each data point represents a mean (\pm SEM) of three independent experiments. Two-way ANOVA is performed on the AUC values of the inhibitor in combination with AraC versus AraC as a single treatment, for both genotypes ($*P < 0.05$, $**P < 0.01$, $***P < 0.001$, $****P < 0.0001$). Absolute IC_{50} values in wild-type cells were 35.9 nM for AraC only versus 15.7 nM in combination with 2 mM CCT251921 and 69.2 nM for only AraC and 19.6 nM for the combination in *IKZF1*^{-/-} cells. (G) Synergy scores generated by Synergy finder software, using the values from Figure 5F.

lower hENT1 expression. The expression of this transporter is rate-limiting for AraC influx,³⁴ particularly at the AraC concentrations that are used in the upfront treatment of BCP-ALL,³⁵ and has been linked to AraC sensitivity in AML³⁶ and BCP-ALL.³⁷ To improve treatment response in this high-risk leukemia subtype, patients might benefit from the selection of alternative nucleoside analogs that rely on the activity of other transporters, such as fludarabine or clofarabine.

In addition to controlling cellular metabolism, *IKZF1* is regarded as a key regulator of lymphoid differentiation³⁸ while loss of *IKZF1* has been associated with stemness.³⁹ In this context, the enhanced expression of the prominent oncogene Evi1 upon loss of *IKZF1* function is intriguing. Evi1 is essential for preventing differentiation of hematopoietic stem cells⁴⁰ and is best known for its role as an oncogene in myeloid leukemia. Overexpression of Evi1 is an independent poor prognostic factor in AML and associated with therapy resistance, including decreased sensitivity to AraC,^{24,41} but the prognostic value of high Evi1 expression in BCP-ALL remains unclear.⁴² We found upregulation of Evi1 mRNA expression upon genetic or pharmacological targeting of *IKZF1* (Figure 4C-E) while BCP-ALL samples displaying high Evi1 expression are enriched for leukemias with *IKZF1* deletion. Although in publicly available chromatin immunoprecipitation-sequencing datasets *IKZF1* does not seem to bind the *MECOM* locus directly,⁴³ there are clear suggestions of a genetic interaction. Despite the fact that *IKZF1* aberrations are less common in AML, recurrent mutations are observed in (pediatric) AML and are associated with poor outcome.^{44,45} Moreover, isolated *IKZF1* deletions and monosomy 7 in AML appear to be enriched in Evi1-rearranged leukemias.⁴⁶ Future studies should reveal whether Evi1 is directly suppressed by *IKZF1* or whether the induction of Evi1 expression upon *IKZF1*

loss is an indirect effect of the stem cell phenotype that is promoted by *IKZF1* loss.³⁹ Moreover, the functional consequences of elevated Evi1 expression in *IKZF1*-deleted leukemias and whether high Evi1 mRNA expression can serve as a potential biomarker for poor outcome in BCP-ALL remain to be established. Our model cell lines do not tolerate modulation of Evi1 itself, suggesting that this protein plays an important role in cell survival and/or proliferation. Although Evi1 itself is not targetable, we showed that inhibition of the upstream kinase CK2, a prominent hit in the CRISPR/Cas9-based loss-of-function screen, which normally phosphorylates and activates both Evi1 and *IKZF1*,^{29,31} can reverse *IKZF1*-loss induced resistance to AraC. Considering our finding together, it is an attractive hypothesis that the resistance phenotype of *IKZF1*-deleted BCP-ALL and high expression of Evi1 are, at least in part, due to a genetic or functional interaction between *IKZF1* and Evi1.

Therapy resistance remains a formidable challenge in the treatment of cancer patients. In this study we identified multiple targetable mechanisms that may overcome drug resistance caused by loss of the tumor suppressor *IKZF1*. Consistent with our previous observations,⁹ we found that targeting the MAPK pathway not only reverses glucocorticoid resistance but also increases sensitivity to AraC in *IKZF1*-deleted leukemia. Additionally, we found that targeting CK2, the upstream activator of both *IKZF1* and Evi1, may represent an Achilles' heel for *IKZF1*-mediated multidrug resistance. Although this clinically approved small molecule inhibitor is not yet used in the treatment of BCP-ALL, a quick translation to clinical application in BCP-ALL seems feasible.⁴⁷ Another promising combination therapy involves drugs targeting the mediator kinases CDK8/19. Importantly, the sensitizing effects of these inhibitors are not limited to *IKZF1*-deleted cells, but

also enhance AraC response in wild-type cells. Of note, CDK8/19 inhibitors are under clinical investigation for the treatment of AML, albeit currently as a single agent.⁴⁸ Therefore this combination therapy is not limited to BCP-ALL but could also be applied in the treatment of other malignancies such as AML, in which AraC is a cornerstone drug playing a crucial role in achieving remission.⁴⁹ Future *in vivo* experiments will have to demonstrate which of the identified targeted therapies would be most effective in reversing therapy resistance in *IKZF1*-deleted BCP-ALL. In conclusion, our study shows that loss of *IKZF1* induces resistance to AraC in BCP-ALL. The high-risk group of patients with this loss may, therefore, benefit from alternative treatment strategies that either replace AraC or combine AraC with small molecule inhibitors that can re-sensitize cells to treatment.

Disclosures

No conflicts of interest to disclose.

Contributions

BMTV designed and performed experiments, analyzed and interpreted the data and wrote the manuscript. MB designed and performed the experiments reported in Figure 1 together with BMTV. LTvdM and FNvL initiated the project and supervised the work. KG analyzed datasets presented in Figures 3G and 4A-C, G as well as Online Supplementary Figures S4 and S5. DSvIS performed experiments presented in Figures 1F, G and 2A, B and Online Supplementary Figures S2 and S3. TMT supported data interpretation and the experimental design reported in Figures 1-5. LL performed and interpreted the experiment presented in Figure 3A, supervised by ADRH. JMB supported analyses of the data presented in Figures 3G and 4G and Online Supplementary Figures S4B and S5D, E. BCB and JPB provided patients' material used in the experiments presented in Figure 1F, G and Online Supplementary Figure S2. VHJvdV, PMH, and

RPK performed analyses and supervised the work presented in Figure 2C-E.

Acknowledgments

We are grateful to Didier Trono for providing psPAX2 (Addgene plasmid # 12260) and pMGD2 (Addgene plasmid # 12259). The pL-CRISPR.EFS.GFP and pLKO5.sgRNA.EFS.tRFP were a gift from Benjamin Ebert (Addgene plasmids # 57818 and 57823). The Human CRISPR enriched pooled library was a gift from David Sabatini & Eric Lander (Addgene #51044). We acknowledge the Utrecht Sequencing Facility (USEQ) for providing sequencing services and data. We acknowledge Ruud Delwel, Leonie Smeenk and Marije Havermans for lively discussions about *Evi1* and providing us with the K562 t(3::8) cells. We are grateful to the flow cytometry facility of the Princess Máxima Center and to the PRIME team of the Radboudumc animal facility for providing technical support.

Funding

This work was supported in part by research funding from the Dutch Cancer Society (KWF) (grants #10072, #11249 and #14659) and from Kika (grant #333). The Utrecht Sequencing Facility (USEQ), which provided sequencing services and data for this study, is subsidized by the University Medical Center Utrecht and the Netherlands X-omics Initiative (NWO project 184.034.019).

Data-sharing statement

RNA sequencing data generated in this study are publicly available in the Gene Expression Omnibus at GSE234637, as are the patients' expression data via reference number GSE87070. The corresponding patients' *IKZF1* status can be found in Online Supplementary Table S1. For R-scripts or any other material requests, please contact F.N.vanleeuwen@prinsesmaximacentrum.nl

References

1. Reedijk AM, Coebergh JWW, de Groot-Kruseman HA, et al. Progress against childhood and adolescent acute lymphoblastic leukaemia in the Netherlands, 1990-2015. *Leukemia*. 2021;35(4):1001-1011.
2. Dixon SB, Chen Y, Yasui Y, et al. Reduced morbidity and mortality in survivors of childhood acute lymphoblastic leukemia: a report from the childhood cancer survivor study. *J Clin Oncol*. 2020;38(29):3418-3429.
3. Pieters R, de Groot-Kruseman H, Van der Velden V, et al. Successful therapy reduction and intensification for childhood acute lymphoblastic leukemia based on minimal residual disease monitoring: study ALL10 from the Dutch Childhood Oncology Group. *J Clin Oncol*. 2016;34(22):2591-2601.
4. Mullighan CG, Su X, Zhang J, et al. Deletion of *IKZF1* and prognosis in acute lymphoblastic leukemia. *N Engl J Med*. 2009;360(5):470-480.
5. Kuiper R, Waanders E, Van Der Velden V, et al. *IKZF1* deletions predict relapse in uniformly treated pediatric precursor B-ALL. *Leukemia*. 2010;24(7):1258-1264.
6. Steeghs EM, Boer JM, Hoogkamer AQ, et al. Copy number alterations in B-cell development genes, drug resistance, and clinical outcome in pediatric B-cell precursor acute lymphoblastic leukemia. *Sci Rep*. 2019;9(1):4634.
7. Yu J, Waanders E, van Reijmersdal SV, et al. Upfront treatment influences the composition of genetic alterations in relapsed pediatric B-cell precursor acute lymphoblastic leukemia. *Hemasphere*. 2020;4(1):e318.
8. Marke R, Havinga J, Cloos J, et al. Tumor suppressor *IKZF1* mediates glucocorticoid resistance in B-cell precursor acute lymphoblastic leukemia. *Leukemia*. 2016;30(7):1599-1603.

9. Butler M, Vervoort BM, van Ingen Schenau DS, et al. Reversal of *IKZF1*-induced glucocorticoid resistance by dual targeting of AKT and ERK signaling pathways. *Front Oncol.* 2022;12:905665.
10. Van der Velden V, Cazzaniga G, Schrauder A, et al. Analysis of minimal residual disease by Ig/TCR gene rearrangements: guidelines for interpretation of real-time quantitative PCR data. *Leukemia.* 2007;21(4):604-611.
11. Frisimantas V, Dobay MP, Rinaldi A, et al. Ex vivo drug response profiling detects recurrent sensitivity patterns in drug-resistant acute lymphoblastic leukemia. *Blood.* 2017;129(11):e26-e37.
12. Zhu YX, Braggio E, Shi C-X, et al. Identification of cereblon-binding proteins and relationship with response and survival after IMiDs in multiple myeloma. *Blood.* 2014;124(4):536-545.
13. Bjorklund CC, Kang J, Amatangelo M, et al. Iberdomide (CC-220) is a potent cereblon E3 ligase modulator with antitumor and immunostimulatory activities in lenalidomide- and pomalidomide-resistant multiple myeloma cells with dysregulated CRBN. *Leukemia.* 2020;34(4):1197-1201.
14. Murphy B, Yin H, Maris JM, et al. Evaluation of alternative in vivo drug screening methodology: a single mouse analysis. *Cancer Res.* 2016;76(19):5798-5809.
15. Pieters R, de Groot-Kruseman H, Verwer F, et al. Dutch ALL11 study: improved outcome for acute lymphoblastic leukemia by prolonging therapy for *IKZF1* deletion and decreasing therapy for ETV6::RUNX1, Down syndrome and prednisone poor responders. *Blood.* 2022;140(Supplement 1):519-520.
16. Pieters R, de Groot-Kruseman H, Fiocco M, et al. Improved outcome for ALL by prolonging therapy for *IKZF1* deletion and decreasing therapy for other risk groups. *J Clin Oncol.* 2023;41(25):4130-4142.
17. Galmarini CM, Mackey JR, Dumontet C. Nucleoside analogues: mechanisms of drug resistance and reversal strategies. *Leukemia.* 2001;15(6):875-890.
18. Feng L, Achanta G, Pelicano H, Zhang W, Plunkett W, Huang P. Role of p53 in cellular response to anticancer nucleoside analog-induced DNA damage. *Int J Mol Med.* 2000;5(6):597-604.
19. Galmarini CM, Thomas X, Calvo F, et al. In vivo mechanisms of resistance to cytarabine in acute myeloid leukaemia. *Br J Haematol.* 2002;117(4):860-868.
20. Churchman ML, Evans K, Richmond J, et al. Synergism of FAK and tyrosine kinase inhibition in Ph+ B-ALL. *JCI Insight.* 2016;1(4):e86082.
21. Wieser R. The oncogene and developmental regulator *EVI1*: expression, biochemical properties, and biological functions. *Gene.* 2007;396(2):346-357.
22. Kataoka K, Sato T, Yoshimi A, et al. *Evi1* is essential for hematopoietic stem cell self-renewal, and its expression marks hematopoietic cells with long-term multilineage repopulating activity. *J Exp Med.* 2011;208(12):2403-2416.
23. Bindels EMJ, Havermans M, Lugthart S, et al. *EVI1* is critical for the pathogenesis of a subset of MLL-AF9-rearranged AMLs. *Blood.* 2012;119(24):5838-5849.
24. Masamoto Y, Chiba A, Takezaki T, et al. *EVI1*-positive AML cells show distinct features and high dependency on ETS transcription factor ERG. *Blood.* 2021;138(Supplement 1):784.
25. Lugthart S, Figueroa ME, Bindels E, et al. Aberrant DNA hypermethylation signature in acute myeloid leukemia directed by *EVI1*. *Blood.* 2011;117(1):234-241.
26. Li W, Xu H, Xiao T, et al. MAGECK enables robust identification of essential genes from genome-scale CRISPR/Cas9 knockout screens. *Genome Biol.* 2014;15(12):554.
27. Sharko AC, Lim C-U, McDermott MS, et al. The inhibition of CDK8/19 mediator kinases prevents the development of resistance to EGFR-targeting drugs. *Cells.* 2021;10(1):144.
28. Buontempo F, McCubrey JA, Orsini E, et al. Therapeutic targeting of CK2 in acute and chronic leukemias. *Leukemia.* 2018;32(1):1-10.
29. Song C, Li Z, Erbe AK, Savic A, Dovat S. Regulation of Ikaros function by casein kinase 2 and protein phosphatase 1. *World J Biol Chem.* 2011;2(6):126-131.
30. Song C, Gowda C, Pan X, et al. Targeting casein kinase II restores Ikaros tumor suppressor activity and demonstrates therapeutic efficacy in high-risk leukemia. *Blood.* 2015;126(15):1813-1822.
31. Bard-Chapeau EA, Gunaratne J, Kumar P, et al. *EVI1* oncoprotein interacts with a large and complex network of proteins and integrates signals through protein phosphorylation. *Proc Natl Acad Sci U S A.* 2013;110(31):E2885-E2894.
32. Rogers JH, Gupta R, Reyes JM, et al. Modeling *IKZF1* lesions in B-ALL reveals distinct chemosensitivity patterns and potential therapeutic vulnerabilities. *Blood Adv.* 2021;5(19):3876-3890.
33. Kufe D, Spriggs D, Egan EM, Munroe D. Relationships among Ara-CTP pools, formation of (Ara-C) DNA, and cytotoxicity of human leukemic cells. *Blood.* 1984;64(1):54-58.
34. Wiley J, Jones S, Sawyer W, Paterson A. Cytosine arabinoside influx and nucleoside transport sites in acute leukemia. *J Clin Invest.* 1982;69(2):479-489.
35. Peters G, Schornagel J, Milano G. Clinical pharmacokinetics of anti-metabolites. *Cancer Surv.* 1993;17:123-156.
36. Candelaria M, Corrales-Alfaro C, Gutiérrez-Hernández O, et al. Expression levels of human equilibrative nucleoside transporter 1 and deoxycytidine kinase enzyme as prognostic factors in patients with acute myeloid leukemia treated with cytarabine. *Chemotherapy.* 2016;61(6):313-318.
37. Ronald W, den Boer M, Meijerink J. Differential mRNA expression of Ara-C metabolizing enzymes explain Ara-C sensitivity in MLL gene-rearrangements infant acute lymphoblastic leukemia. *Blood.* 2003;101(4):1270-1276.
38. Marke R, van Leeuwen FN, Scheijen B. The many faces of *IKZF1* in B-cell precursor acute lymphoblastic leukemia. *Haematologica.* 2018;103(4):565-574.
39. Li Z, Li S-P, Li R-Y, et al. Leukaemic alterations of *IKZF1* prime stemness and malignancy programs in human lymphocytes. *Cell Death Dis.* 2018;9(5):526.
40. Kataoka K, Sato T, Yoshimi A, et al. *Evi1* is essential for hematopoietic stem cell self-renewal, and its expression marks hematopoietic cells with long-term multilineage repopulating activity. *J Exp Med.* 2011;208(12):2403-2416.
41. Hinai AA, Valk PJ. Aberrant *EVI 1* expression in acute myeloid leukaemia. *Br J Haematol.* 2016;172(6):870-878.
42. Nabil R, Abdellateif MS, Gamal H, et al. Clinical significance of *EVI-1* gene expression and aberrations in patient with de-novo acute myeloid and acute lymphoid leukemia. *Leuk Res.* 2023;126:107019.
43. Ferreirós-Vidal I, Carroll T, Taylor B, et al. Genome-wide identification of Ikaros targets elucidates its contribution to mouse B-cell lineage specification and pre-B-cell differentiation. *Blood.* 2013;121(10):1769-1782.
44. de Rooij JD, Beuling E, van den Heuvel-Eibrink MM, et al. Recurrent deletions of *IKZF1* in pediatric acute myeloid leukemia. *Haematologica.* 2015;100(9):1151-1159.
45. Zhang X, Huang A, Liu L, et al. The clinical impact of *IKZF1* mutation in acute myeloid leukemia. *Exp Hematol Oncol.* 2023;12(1):33.
46. Lavallée V-P, Gendron P, Lemieux S, D'Angelo G, Hébert J, Sauvageau G. *EVI1*-rearranged acute myeloid leukemias are

- characterized by distinct molecular alterations. *Blood*. 2015;125(1):140-143.
47. Grygier P, Pustelny K, Nowak J, et al. Silmitasertib (CX-4945), a clinically used CK2-kinase inhibitor with additional effects on GSK3 β and DYRK1A kinases: a structural perspective. *J Med Chem*. 2023;66(6):4009-4024.
48. Borthakur GM, Donnellan WB, Solomon SR, et al. SEL120-a first-in-class CDK8/19 inhibitor as a novel option for the treatment of acute myeloid leukemia and high-risk myelodysplastic syndrome-data from preclinical studies and introduction to a phase Ib clinical trial. *Blood*. 2019;134(Supplement_1):2651.
49. Cros E, Jordheim L, Dumontet C, Galmarini CM. Problems related to resistance to cytarabine in acute myeloid leukemia. *Leuk Lymphoma*. 2004;45(6):1123-1132.